The University Of Sheffield.

Emulsion Templated Porous Scaffolds for Bone Tissue Engineering

(Edited for online submission)

Priyalakshmi Viswanathan

2nd December 2010

Supervisors: Dr. Giuseppe Battaglia

Dr. Gwendolen Reilly

Submitted to the University of Sheffield in partial fulfilment of the MPhil degree in Materials Science and Engineering

Acknowledgements

I would like to sincerely thank my supervisors Dr. Gwen Reilly and Dr. Beppe Battaglia for all the opportunities and support during my MPhil.

The Battaglia and Reilly group members for constant support and guidance.

Additionally, I would like to thank Dr. Christine Fernyhough, Department of Chemistry, University of Sheffield for the synthesis of PBD-PAA block copolymer.

Dr. Adrian Boatwright, University of Nottingham for the use of the XPS services at Nanotechnology and Nanoscience Centre, funded by the EPSRC open-access scheme.

Dr. Simon Forester, Department of Materials Science and Engineering for XPS analysis.

Dr. Les Coulton, Mellanby Bone Centre, Medical School, University of Sheffield for help with the micro-CT analysis and reconstruction.

List of Abbreviations

hMSC – human mesenchymal stem cell

hESC- human embryonic stem cell

ECM- Extracellular Matrix

RGD- Arg-Gly-Asp peptide sequence

PEG- poly(ethylene glycol) also known as PEO- poly(ethylene oxide)

HIPE- high internal phase emulsion

polyHIPE- polymerized high internal phase emulsion

PS- Polystyrene

DVB- Divinylbenzene

PDI- polydispersity

Span 80- Sorbitan monooleate

PS-PAA- polystyrene-b-poly(acrylic acid)

PS-PEO- polystyrene-b-poly(ethylene oxide)

PBD-PAA- poly(1,4-butadiene)-b-poly(acrylic acid)

Summary

In the human body, cells experience a range of physicochemical properties. Recent research in stem cell differentiation has shed light on how they (and any cell for that matter) respond to their surrounding environment from chemistry and surface chemistry to surface topology and substrate stiffness/elasticity. Additionally, it is well known that cell behaviour is different in 2D compared to 3D. One way of understanding cell behaviour in 3D *in vitro*, is by providing a 3D construct or scaffold, generally a synthetic or biopolymer, in which cells can proliferate in.

Herein, polymer scaffolds were synthesized and characterized. Scaffolds were made by emulsion templating (water-in-oil emulsion) technique, known as high internal phase emulsions (HIPEs). The use of a monomer (styrene) in the oil phase allows for the polymerization in this phase and thus producing porous polymers (foams), which can be used as scaffolds for tissue and cell culture in 3D. Traditional low molecular weight surfactants (sorbitan monooleate) in the emulsion system have been replaced with block copolymer surfactants (polystyrene-b-poly(ethylene oxide), poly(1,4-butadiene)-b-poly(acrylic acid) and polystyrene-b-poly(acrylic acid)) with the aim of controlling the surface chemistry and topology. The scaffold morphologies were characterized by scanning electron microcopy (SEM), confocal laser scanning microscopy (CLSM) and micro x-ray computational tomography (micro-CT). To assess the scaffold surface chemistry, X-ray photoelectron spectroscopy (XPS) and contact angle measurements were carried out. The results obtained thus far suggest that block copolymers can used as effective surfactants in the emulsion process. While synthesis parameters need to be optimized and controlled, porous (but not always interconnecting) foams were produced. XPS and contact angle measurements revealed that the surface functionality provided by the block copolymers (poly(acrylic acid) moieties) are retained post synthesis and purification of the foams. This bodes very well to the engineering of *ad hoc* functionalized scaffold for stem cell engineering applications

1. Introduction

1.1 Tissue engineering and regenerative medicine

Regenerative Medicine is the manipulation or the "engineering" of living cells to restore or replace physiological functions of damaged organs that cannot heal themselves. The engineered cells, either taken from the same patient (autologous) or from donors (exogenous), often require the aid of a scaffold that support cell functions toward the regeneration of the tissue. Such a field also known as Tissue Engineering involves scientists, clinicians and engineers across the spectra of medicine, biology, materials science, chemistry and physics.

1.1.1 Stem cells in tissue engineering

One appropriate source of cells is the use of stem cells. These are uncommitted cells that are capable of differentiating into several cell phenotypes. Stem cells can be pluripotent (i.e. able to develop into more than one type of mature cell) or multipotent (i.e. able to develop into closely related family of cells). A common example of pluripotent stem cells are Embryonic stem cells (ESC). These are derived from the blastocyst, which are a small cluster of cells formed few days after fertilization. These cells have the potential to develop into almost any cell type found in the body. However multipotent cells lack of the flexibility of ESCs, they are more accessible as they are conserved during the body development into pocket of cells known as niches, indeed they are often refereed as adult stem cells. Example of multipotent stem cells Mesenchymal stem cells (MSCs). These are derived from bone marrow, have shown to differentiate into bone[1], cartilage[2] and muscle[3]. Although subject to discussion, they can also differentiate into nerve cells[4].

1.1.2 3D scaffolds in tissue engineering

In order to maintain cell-matrix interactions, the choice of an appropriate scaffold, depending on the application, is required. There are many naturally derived scaffolds available such as Matrigel™(extracellular matrix components extracted from mouse tumours), used *in vitro* cell culture studies, that provide the right environment for cellular function however, their complex composition and batch-to-batch variability

hinder experimental reproducibility. It also limits us from understanding cell-matrix and cell-cell interactions. Other natural ECM-based matrices such as collagen[5] and fibrin have also been employed in wound healing and tissue sealants[6]. To achieve better control over cellular response for specific tissue type, synthetic polymers have been proposed. Several synthetic biocompatible and biodegradable polymers have approved by the Food and Drug Administration for *in vivo* applications. These include, poly(caprolactone), poly(ethylene oxide), poly(vinyl alcohol), poly(acrylic acid), poly(2-hydroxy ethyl methacrylate) to name a few. In order for scientists to effectively use these starting materials and synthesize 3 dimensional networks with the appropriate physical and chemical cues needed for desired cellular response, they must first understand the properties of a cell's natural environment-the extracellular matrix.

1.2 ECM structure and function

Cells are inherently sensitive to their microenvironment. For a cell to sense its matrix, it must first pull against it, then it must convert that information by activation of specific signalling pathways for the cell to generate a force to deform the matrix and subsequently regulate eventual cellular processes such as proliferation, motility differentiation and/or apoptosis. For this reason, an understanding of exctracellular matrix (ECM) structure, composition and function is necessary. The ECM consists of meshwork of proteins including collagen, fibronectin, laminin, elastin as well as several glycosaminoglycans (GAGs). Collagen and elastin are fibrous and are known to provide structural support for the cells while other non fibrous components such as the GAGs modulate the binding and activity of growth factors[7]. Cell-matrix interactions and adhesions are governed by cell surface receptors known as integrins. These are heterodimeric transmembrane protein consisting of a large α subunit and a smaller β subunit. By combining various α and β subunits, 24 different heterodimers may be formed that determine ligand binding specificity. Integrins work alongside other adhesion mediating transmembrane proteins such as cadherins (calcium dependent adhesion) and selectins. Concomitantly, ECM proteins consist of ligands or domains that aid the binding of cell surface receptors. The most well known of these is the RGD (Arg-Gly-Asp) peptide, reported first by Ruoslhati[8], as a cell attachment epitope, present in fibronectin and similar proteins. Cells continually remodel and restructure their microenvironment. Although most cells reside in a state of

homeostatis *in vivo*, some cells undergo physiological changes (like those of the mammary glands) during development[9]. This requires the need to remodel the ECM in order to maintain tissue function. This is achieved via secretion of ECM proteases such as metalloproteinase (MMP) and enzymes such as hyaluronidases[9]. Although ECM composition varies from tissue to tissue, a knowledge of its general composition enables scientists to effectively design and synthesize novel 3D scaffolds.

1.3 Manipulating Regulation of Chemical Signals

Molecular regulatory signals (and chemical gradients) such as growth factors secreted by cells, the ECM or added into *in vitro* studies are extremely important in cellular fate processes. From embryogenesis through adulthood, this is highly controlled in space and time.[10, 11] For example, human ES cell pluripotency and differentiation states maybe controlled by colony size using micropatterned substrates of ECM islands.[12] Large islands (hence colonies) maintained pluripontency by increased level of Smad1 inherent in hES cells (Figure 1- Deleted for online submission due to copyright restrictions). This increased levels of the Smad1 antagonist, growth differentiation factor (GFD3) while maintaining constant levels of bone morphogenic protein-2 (BMP-2). This resulted in decreased levels of phosphorylated Smad1, thus increasing pluripotency. Recent advances in fabrication of 3D microfluidic devices from collagen, agarose and alginate have also allowed the regulation of chemical gradients within the scaffold by continuously washing away secreted factors while perfusing known concentrations of active factors.[13] Biochemical regulation however, is not limited to soluble factors. Matrix chemistry may be manipulated by changing adhesion properties. For example, ECM ligand distribution was enhanced by attaching ligands to fibronectin matrices specific for the integrin $\alpha 5\beta 1$ resulting in osteobalst specific differentiation of hMSCs[14]. Adhesive ligand density as well as spacing has shown to affect other cellular processes such adhesion and spreading.[15] MC3T3 mouse osteoblasts, 3T3 fibroblasts and B16-melanocytes were grown on cell inert poly(ethylene glycol) (PEG) surfaces patterned with Au nanodots functionalized with cyclic RGD motifs. Cell spreading (via integrin clustering and activation leading to focal adhesion formation) and proliferation was enhanced on surfaces with nanodot spacings of 58 nm compared to a spacing of 73nm, where poor cell spreading lead to eventual apoptosis.[15] This sensitivity perhaps arises from mimicking *in vivo* such as the 67nm banding structure found in collagen fibrils.[16] Even synthetic functional

groups such as methyl and carboxylic acids moieties coated on clean glass (by silane modification) directed hMSC differentiation. Methyl modification promoted proliferation and maintained MSC phenotype, while carboxylic acid surfaces promoted chondrogenic differentiation in the absence of chemical stimuli.[17]

1.4 Manipulating Regulation of Biomechanical and Structural Signals

Biomechanical signals that cells sense in their extracellular environment are those that are associated with changes in cellular morphology (cellular deformation) by means of compression, mechanical stress or shear. As such, cellular morphology (or rather a deviation from 'normal' cellular morphology) is one obvious indicator and regulator of the physical effects of cellular function such as differentiation and lineage commitment.[18] Each cell type is associated with a unique morphology that relates to its specific function. For example osteoblasts are large and polygonal, chondrocytes are small and rounded and myoblasts are medium sized and spindle like. Many cells types make different fate decisions such as growing, differentiating or dying depending on adhesivity or mechanical compliance of the matrix.[11] This can be achieved by topographical control of the substrate by creating islands, pits, groves and ridges[19, 20] with defined size (nm to μm scale) and shape. For example, Dalby et. al. investigated nano topographies (pits) and its spatial orientation by electron beam lithography to study osteogenic differentiation of human mesenchymal stem cells (hMSCs) in the absence of osteogenic inducing supplements (Figure 1- deleted for online submission due to copyright restrictions).[20] Nano sized pits on substrates were ordered (square and hexagonal arrays), highly disordered (random array) and controlled disordered (± 50nm from the true centre of a square array). Osteogenic marker proteins such as osteocalcin and ostepontin were expressed in large quantities on slightly disordered array compared to the square array or completely random array. Besides the effects of nano topographical features presented, the order (and disorder) was detrimental to osteogenic differentiation. This suggested that the patterned substrate modulation of adhesion formation and cell spreading is a factor that dictates MSC fate. Changes in cell adhesion as a result of nano patterning has direct consequences in a cell's cytoskeletal tension, as adhesions form anchor points of the cytoskeleton.

Matrix physical properties such as elasticity and regulation of chemical pathways work synergistically to influence cell shape and eventual fate. Human MCSs cultured on substrates of similar rigidities, with cell-substrate contact controlled by the size of the adhesive patterns lead to adipogenic and osteogenic differentiation based on pattern size.[1] Small islands, which maximize matrix contact, incurred adipogenesis while large islands, which maximize cytoskeletal contractility lead to osteogenesis. The mechanism by which cytoskeletal tension and shape dependent lineage commitment is said to be regulated by the RhoA signalling pathway.[1, 21] RhoA is small protein member of the Rho family of GTPases involved in cell signalling and cytoskeltal organization. Engler et. al. showed that MSC's cultured on poly(acrylamide) gels of various stiffness by varying the cross-linking density, exhibited controlled stem cell differentiation and lineage commitment.[22] Cells grown on soft gels that mimic the brain (~1 kPa) expressed early neuronal cytoskeleton markers, β-tubulin, cells cultures on stiff gels (~11 kPa) like that of muscle expressed early myogenic transcription factors MyoD, and rigid gels like pre calcified bone (~34 kPa) expressed the osteogenic transcription factor CBFα-1.[22]

1.6 Scaffold design criteria

A scaffold is a 3-dimensional structural support consisting of an interconnecting porous network in which cells can survive and proliferate as they would under physiological conditions. Different tissues require different scaffold mechanical strength. A scaffold essentially acts as the cell extracellular matrix (ECM) and it is imperative that the scaffold provides sufficient ECM-cell type and cell-cell interactions and thereby maintains the morphology and integrity of the cell. Not only do the cells need to survive, the scaffold should facilitate cell access to nutrients and removal of metabolic wastes by appropriate porosity or permeability. For clinical applications, the scaffold should be biocompatible i.e. non-toxic and non-immunogenic and biodegradable at a controllable rate preferably coordinated with the

rate of tissue repair or growth *in vitro* and *in vivo.*[23-26] It can be predicted that the ideal synthetic scaffold should mimic the complexities of the ECM in order to maintain appropriate cell- matrix and cell-cell interactions and signalling pathways. It is evident from the aforementioned work that there are many cell-matrix cues and stimuli that influence stem cell differentiation. However, literature to date study individual cues. Whether it is the use of growth factors, ECM structure, or chemical composition, these studies show that the ECM alone is not sufficient to promote full differentiation to that of a mature adult.[27] Synthetic scaffolds must incorporate the range of length scale of features (10 nm – 100 μm) that cells experience in vivo Scaffold architecture such as pore diameter affects growth of specific cell types; 380 μm - 405 μm supported osteoblast and chondrocyte growth while 290 μm -310 μm supported fibroblasts.[28] Even nanoscale roughness (by means of salt leaching) on poly(L-lactic acid) scaffold pore edges has shown to increase cell attachment and expression of ECM components.[29] Additionally, they must have the right mechanical properties and allow for the incorporation of biochemical signals that are regulated in 3D. For example, hydrogels constitute a popular class of biomaterials, the physical properties of which are easily tunable. Burdick et. al. were able to synthesize methacrylated hyaluronic acid hydrogels whose elastic moduli were spatially controlled by UV curing and therefore creating local mechanical gradients, mimicking an aspect of MSC niche.[30] Human MSCs cultured on these hydrogels exhibited spreading and proliferation behaviour correlating to the mechanical gradients, with increased spreading on stiffer areas and poor spreading on softer areas. Hydrogels have also been chemically patterned in 3D.[31] Here, agarose hydrogels were modified with a 2-nitrobenzyl protected cystein, yielding free thiol groups when exposed to conventional He/Ne laser source making them reactive towards maleimide-terminating peptides. As a result, a 3 dimensional peptide functionality was localized in a confined volume which has applications in enhancing nerve guidance.[32] Aligned and random fibrous scaffolds made by electrospinning with tailored fibre diameters from the micro- to nano length scales have also been used to guide cell migration and proliferation.[33, 34] Given the diversity of fibril tissue structures such as tendon (aligned and non aligned) and bone (concentric weaves), makes electrospun fibres particularly suited for these tissues. Furthermore, fibrous scaffold scaffolds made from poly(caprolactone) have also been used to direct hES differentiation into neuronal

lineages and promote neurite outgrowth.[35] Other strategies, such as emulsion templating will be discussed in detail below.

1.7 Emulsion Templating

A proposed method for fabricating porous polymers is by emulsion templating. A high internal phase emulsion (HIPE) is used. In the HIPE system, the internal or droplet phase volume fraction (ϕ) is greater than 0.7405.[36] This is the volume at which droplets are still spherical and are packed in the most efficient manner. Above this volume, droplets adopt a polyhedral geometry, or more likely in real systems become polydisperse. The concentrated droplets are separated by a thin film of the continuous phase. When the continuous phase consists of a monomer that is subsequently polymerized by radical initiation and the droplet phase evaporated, a polyHIPE or a porous polymer is formed. One of the well studied systems is water-in-oil (w/o) HIPES where the oil phase consists of styrene and crosslinked with divinylbenzene and the aqueous phase consists of a water soluble radical initiator solution.[37, 38] In a w/o polymerized HIPE, a hierarchy of porosity in the resulting foams is present. Large pores are created due to the loss of water termed as voids. Within each three dimensional void, smaller pores exist, termed windows or interconnects which are responsible for the interconnectivity between adjacent droplet that results in 'open cell' foams (Figure 2)

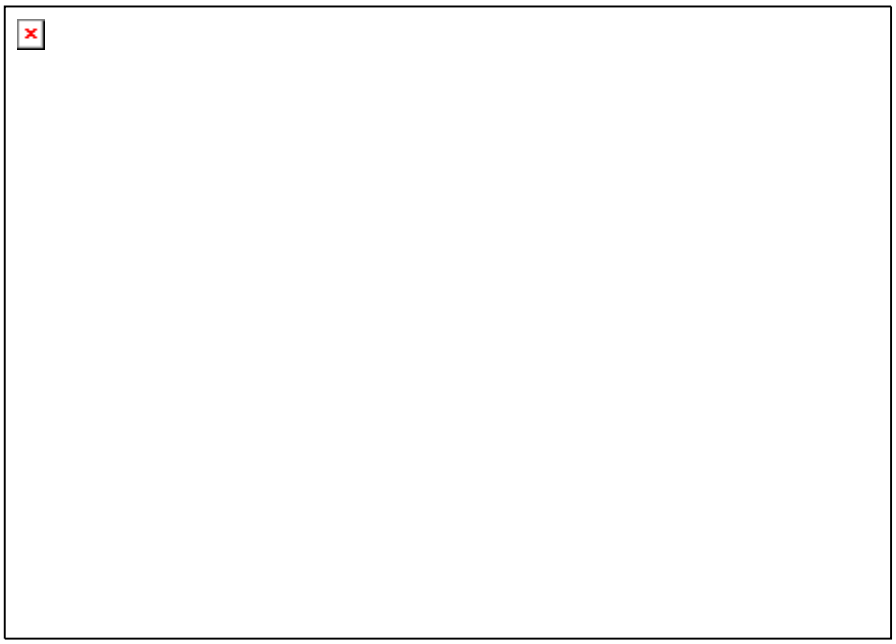

Figure 2. Typical scanning electron micrograph of a polyHIPE. a) Low magnification b) High magnification showing void and interconnect formation. c) High magnification showing structure of PS matrix. Scale bars: a) 50 μm, b) 10 μm and c) 5 μm

1.8 Controlling HIPE Morphology and Stability

PolyHIPE morphology is controlled by the various parameters involved in the emulsion process. The first and most important parameter is the choice of surfactant, its chemical nature and concentration. For a non-ionic surfactant, the HLB (hydrophilic-lipophilic balance) is an important factor in deciding whether it is suitable for a particular type of emulsions. Surfactants with low HLB values (ideally 2- 6) are more oil soluble and so suitable for w/o systems. The most common surfactant used for w/o emulsions non ionic fatty acid esters such as sorbitan monooleate (Span 80). However, ionic surfactants such as cetyltrimethylammonium bromide (CTAB), dodecylbenzenesulphonic acid (DDBS) or a combination of surfactants have also been used.[40, 41]

1.9 Applications of polyHIPEs in tissue engineering

Since the patenting of polyHIPEs in the 1980's by Unilever, they have been used for various applications including their use as 3D scaffolds for cell culture.[42-44] A variety of cell types have been grown on polyHIPEs and show preferential growth in 3D compared to 2D environments. Primary rat osteoblasts grown on styrene/DVB polyHIPEs with porosities ranging from 40μm to 100μm showed that cells were able to maintain not only their osteoblast phenotype but mature over the course of cell culture expressing greater levels of osteopontin and osteocalcin[45, 46] in 3D compared to cells grown in 2D tissue culture plastic. Similarly MG63 human osteosarcoma cells cultured for a maximum of 35 days survived, proliferated and expressed greater levels of alkaline phosphatase activity and osteocalcin expression, cultured on polyHIPEs compared to cells cultured in 2D[47]. Phosphatase is an enzyme that hydrolyses phosphate ester groups resulting in the release of phosphates. Alkaline phosphatase (ALP) is bound to the membrane of osteoblasts and enhances osteogenesis by degrading pyrophosphates. Pyrophosphates inhibit calcium crystallization and deposition of inorganic phosphates. Therefore, ALP is an early marker for osteogenesis. Additionally, polyHIPEs coated with hydroxyapatite, were able to remarkably increase depth of cell penetration into the scaffold by as much as 44%.

Human embryonal stem cells from the TERA2.cl.SP12 embryonal carcinoma stem cell line showed enhanced neurite outgrowth on laminin coated polyHIPES with complex and more extensive neural networks forming in comparison to 2D culture.[39] Analysis of protein expression showed that cells grown in both 2D and 3D, generally showed presence of maturing, post-mitotic neuronal phenotypes neuroD and MAP2ab but proteins expressed in developing nervous systems (MAP2c, nestin) were only present in cells grown in 3D. It is important to note that in these studies, cell were cultured in excess of 30 days and showed no toxicity due to the polyHIPE material showing enhanced cell activity in comparison with 2D indicating that a 3D environment or construct may help scientists understand better biological behaviour *in vivo*.

Emulsion templated scaffolds have also found a niche in other biological applications, e.g., HepG2 liver cells grown on polyHIPE scaffolds were subjected to the drug methotrexate, a known cytotoxin (Figure 3- Deleted for online submission due to copyright restrictions).[48] Drug metabolism by the liver cells grown on the scaffolds showed that cells were much more resistant to higher concentrations of methotrexate than cells grown on 2D surfaces, concluding that polyHIPEs were suitable not only for cell culture but also as a 3D model for drug screening.

1.10 Emulsion templating- advantages and limitations

Emulsion templated porous polymers have shown to be promising scaffolds. Their physical properties are easily tunable, for example, reaction parameters such as rate of stirring, aqueous phase addition, temperature and the use of inert porogens can be optimized to produce the desired scaffold morphology. Varying the crosslinking density and the use of viscoelastic monomers such as ethylhexyl acrylate and ethylhexyl methacrylate[49, 50] allow for the tuning of desired mechanical properties of the scaffold. Additionallly, polyHIPE based scaffolds have been made biodegradable and biocompatible by using poly(lactic acid co-glycolic acid)[51], poly(caprolactone)[52] and poly (propylene fumerate)[53] making them relevant for clinical applications. However, such scaffolds as with many other synthetic systems in tissue engineering do not incorporate the range of features from the micro to nano scale physical cues and well as chemical cues present in the extracellular matrix. Efforts have been made to functionalize polyHIPE scaffolds using plasma polymerization[54] and polymer grafts by Huisgen type ‘click’ chemistry[55]. However, two-step post synthesis modifications often lack control over 3 dimensional functionalization and reproducibility.

1.11 Block copolymers as surfactants

Advances in controlled polymerization techniques have allowed for the design of ‘macro’ or polymeric surfactants based on block copolymers[56]. Block copolymer

surfactants can have molecular weights several orders of magnitude higher than conventional surfactants. In solution, amphiphilic block copolymers behave in very similar ways to their low molecular weight counterparts.[57] They have recently gained popularity in their properties as surfactants in emulsion polymerization.[58, 59] However, their uses in emulsion technology have been mainly limited to o/w emulsions to form latexes. Some literature exists in their use as o/o emulsion to form porous polymers[60] but both these emulsion systems are limited to the use of Pluronic type (Poly(ethylene oxide)-b-poly(propylene oxide)-poly(ethylene oxide) tri- block copolymer surfactants that are extensively used in various industrial applications. Review of the literature is scarce with regards to their use in w/o emulsion systems, EB (poly(ethylene oxide)-b-poly(butylene oxide)) block copolymers have been shown to stabilize polyHIPEs with a higher surfactant efficiency (minimum of 0.125 wt/wt% of the organic phase) than Span 80.[61] Of particular interest in this case were polymerizable surfactants, i.e. block copolymers that have a reactive end group, enabling them to be incorporated into the backbone of the resulting polyHIPE.

It is well known that the surfactants such as Span 80 and other small molecule surfactants are washed away during the purification[61, 62] of the polyHIPE materials exposing the polymerized continuous phase (e.g. polystyrene/divinylbenzene). We therefore herein propose a new approach to synthesize polyHIPEs using block copolymers as surfactants. The intrinsic macromolecular nature of the copolymer will guarantee that they remain anchored after HIPE polymerization, enabling control over both surface chemistry and topology. The block copolymers chosen here are polystyrene-b-poly(ethylene oxide) (PS-PEO), polystyrene-b-poly(acrylic acid) (PS-PAA) and poly(1,4-butadiene)-b-poly(acrylic acid) (PBD-PAA). Additionally, the unfavourable thermodynamic mixing of block copolymer mixtures, for example, between PS-PEO and PS-PAA, will drive their micro-phase separation at the oil-water interface. This will be exploited by subsequent polymerization to trap their configuration and produce well-defined domains of the hydrophilic blocks (PEO and PAA) on the surface of the foams in 3D. Such phase separation has been previously observed in block copolymer vesicles.[63] If such phase separation can occur in bilayer systems, then it is predicted that this will also be observed in a monolayer system at the oil-water interface present in HIPEs.

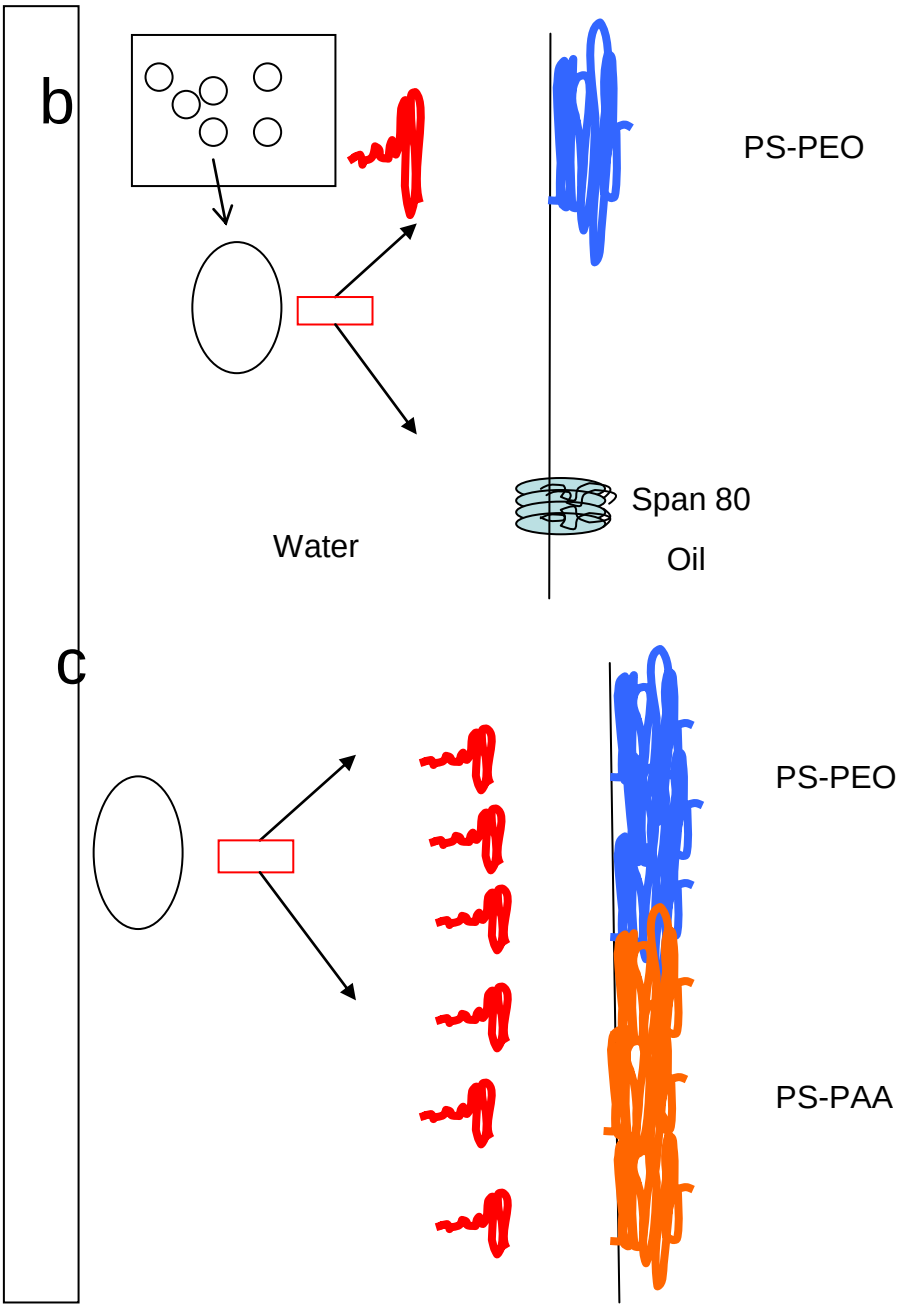

Figure 4. a) Deleted for online submission due to copyright restrictions. Transmission electron micrographs of micro-phase separated PMPC-PDPA and PEO-PDPA polymersomes, selectively stained for PMPC-PDPA. Adapted from Ref 60. b) Schematic of water-in-oil emulsions and surfactant assembly at the interface. PS-PEO and Span 80 shown as examples and c) Predicted micro-phase separation of PS-PAA and PS-PEO block copolymers at the oil-water interface. Size and pattern of domains formed will be based on the molar ratio of the two block-copolymers.

2. Materials and Methods

2.1 Materials

The monomers styrene (99%, Sigma Aldrich), divinylbenzene (80% in mixture, the rest being m- and *p*-ethyl styrene, SigmaAldrich), were passed through a basic alumina (Fluka, Brockmann activity I) column to remove the inhibitor; *p*-tert butlycatechol.

Potassium persulfate(Sigma Aldrich), calcium chloride dihydrate (Sigma Aldrich), polystyrene-b-poly(ethylene oxide) (Mw= 22500-27500 g/mol, PDI = 1.1-1.3, Sigma Aldrich), Poly(Styrene)-b-poly(acrylic acid) (Mw= 8100-8500 g/mol, PDI=1.1-1.3, Sigma Aldrich)) Span 80(Sorbitan monooleate, Sigma Aldrich) and poly(butadiene)-b-poly(acrylic acid) (Mw=3000 g/mol, PDI =1.02, (provided by Dr. Christine Fernyhough, Department of Chemistry, University of Sheffield) were all used as received.

The polymers poly(styrene)-b-poly(ethylene oxide) and poly(styrene)-b-poly(acrylic acid) were synthesized by ATRP and poly(butadiene)-b-poly(acrylic acid) was synthesized by anionic polymerization.

2.2 Methods

2.21 Scaffold Preparation with Span 80

All foams prepared were 90% porous based on aqueous phase volume and have been described extensively in literature. The organic phase (ϕ=0.1) of styrene (80 wt/wt%), divinylbenzene(DVB) (20 wt/wt%) and the surfactant Span 80 (10, 20,30,40 and 50 wt/wt%) relative to the organic phase was charged in a glass beaker fitted with an overhead mechanical stirrer and was stirred constantly at 500 rpm. The aqueous phase consisting of a solution of potassium persulfate (1 wt/v%) in distilled water was added drop wise to the organic phase using a peristaltic pump at a rate of 5 ml/min forming a highly viscous and white emulsion. Once addition was complete, the resulting HIPE was stirred for a further minute to homogenize, then transferred to a glass vial and polymerized in an oven at 60°C for 24 hours to produce a foam. Extraction of this foam was carried out in a soxhlet apparatus for 24 hours in propan-2-ol. The foams were then dried in vacuum at room temperature overnight to remove

all solvent residues. To expose the pores on all sides, the edges of the foam were finely shaved with a razor blade.

For scaffolds where the crosslinking density was varied, the surfactant concentration, Span 80 was kept constant at 20 wt/wt% and the crosslinking concentration of DVB was varied from 10-50 wt/wt%.

2.22 Scaffold Preparation with block copolymer surfactants

Poly(butadiene)-b-poly(acrylic acid) (PBD-PAA), Poly(styrene)-b-poly(ethylene oxide) (PS-PEO), Poly(styrene)-b-poly(acrylic acid)

For scaffolds with single block copolymer, all foams prepared were 80% porous based on aqueous phase volume. At volumes fractions higher than 0.8, phase separation at all surfactant concentrations attempted. The ratio of monomer: surfactant was maintained at 15000:1 for PBD-PAA and $2.5x10^4$:1 for PS-PAA and PS-PEO. PS-PAA was first dissolved in tetrahydrofuran before solubilizing in the monomer. Divinylbenzene alone was used as the monomer as the introduction of styrene increased emulsion instability leading to rapid phase separation. The aqueous phase consisting of 0.1 wt/wt % of the initiator $K_2S_2O_8$ adjusted to pH 10 with 1M NaOH was added drop wise to the oil phase (DVB and surfactant) using a peristaltic pump at a rate of 10ml/min. Once the aqueous phase was added, the resulting emulsion was stirred for a further 5 minutes to homogenize. The emulsion was polymerized in an oven at 60 °C for 24 hours. The resulting foam was then extracted in a soxhlet for 48 hours using a 50/50 v/v% of deionized water / isopropanol.

Emulsions with mixed block copolymer formulations using PS-PEO and PS-PAA were also prepared. As before, the molar ratio of monomer : surfactant was kept constant at $2.5x10^4$:1.. For convenience, the notations for block copolymer mixtures will be referred as PEO for PS-PEO, PAA for PS-PAA. The molar ratio of PS-PEO and PS-PAA was varied in the following ratios PEO 100, PEO 75:PAA 25, PEO 50:PAA 50, PEO 25:PAA 75 and PAA 100.

2.23 Scaffold Characterization

Scanning Electron Microscopy Scaffold morphologies were characterized using an SEM. Fractured segments from various parts of the foam were mounted on an

aluminium stub with a sticky carbon pad. Samples were gold coated (approx 15-20 nm) using an Emscope SC 500 A sputter coater unit and viewed with an FEI Inspect F field emission gun scanning electron microscope. Samples were viewed with an accelerating voltage of 20kV. Samples containing block copolymer surfactants were highly sensitive to the electron beam causing significant damage to the samples and were thus viewed with an accelerating voltage of either 1 or 5kV.

Porosities of the scaffolds were measured from SEM micrographs using the image analysis software Image J (NIH Image). A random selection of 50 voids and 100 interconnects were measured from several micrographs of the same foam to obtain a more representative measurements. The assumption that the fracture of the segments exactly bisect the voids is made, which means that the measured values are all underestimates of the true value. Therefore a statistical correction is introduced[41] This is done by evaluating the average of the ratio R/r, where R is the equatorial void diameter and r is the measured diameter on the micrograph (see figure). The statistical factor is calculated using the following formula:

$$h^2 = R^2 - r^2$$

Where the probability of the sectioning takes place at a distance given by h, from the centre of the void is the same for all values of h. This means that the average probability h is R/2. By substituting this in the above equation we get $R/r = 2^{(1/3)}$, which is the statistical correction. By multiplying this number to the measured diameters, a more representative value.

To analyze the topographical effects of PS-PEO foams, semi quantitative methods using the image analysis software Image J was used. For foams synthesized at each temperature at least two high magnification representative micrographs were used. 100 ‘particle’ diameters were measured and plotted as a function of temperature. The same calculations for foams with mixed block copolymer formulations (PS-PEO and PS-PAA) were made and particle diameters was plotted as a function of loss of PS-PEO functionality.

Confocal Laser Scanning Microscopy Scaffold morphology was analysed using a Zeiss LSM 10 META confocal laser scanning microscope using a 10x Neoflar lens. The PS/DVB polymers are auto fluorescent at their maximum in the green region

(488 or 514 nm lasers). All images were then analysed using the image software, Zeiss LSM image viewer.

Micro-Computational Tomography To evaluate the porosity of the scaffolds micro CT analysis was performed using SkyScan 1172 high resolution scanner. Scaffolds with a diameter of 1.4 cm and height of 2-3mm were used. The applied X-Ray voltage was 35kV and no filter was used. The pixel size (resolution) was 1.7μm . A total of 1400 scans were achieved and reconstructed using the SkyScan micro-CT analysis software package. Circular regions of interest (diameter=1.25 mm, height= 0.6 mm) were chosen and 3D models were generated using the adaptive rendering algorithm available in the SkyScan software package which also calculated scaffold open porosity, closed porosity, volume and pore strut thickness.

Contact angle measurements Wettability of the scaffolds was ascertained by contact angle measurements using a Ramé-Hart contact angle goniometer. Between 2-4 μL droplets of DI water (pH 7) and DI water adjusted to pH 2 by using 1M HCl was used. At least three measurements were made for each sample.

X-Ray Photoelectron Spectroscopy (XPS) Surface Characterization by XPS was carried out by Simon Forster, Department of Engineering Materials as follows. Surface analysis was carried out with a Kratos Ultra DLD X-ray photoelectron spectrometer. A monochromated Al Kα X-ray source at a power of 150*W* was used. The spot size was 300μm by 700μm. The pressure in the main ultra-high vacuum chamber was maintained below 1 x 10^{-8}*mbar* for all analyses. Unless otherwise stated, data was collected at an angle of 90° (from the surface). As the polymeric samples analysed in this work are electrical insulators, charge neutralization is required to prevent the build up of positive charge on the surface of the material. An electron flood gun was focused onto the sample to compensate for the positive charging effect. High-resolution spectra of the elemental core level C 1s were also completed to gain an understanding of the carbon environments present on the surface. The parameters used were a binding energy range of 275 to 300*eV,* a pass energy of 20*eV* and a step interval of 0.1*eV.*All data collected was then analysed using CasaXPS software Peaks were again fitted by removing unwanted background using CasaXPS software. Asymmetry of the peaks was fixed at zero and the position of each peak was fixed relative to the hydrocarbon peak. After initial rough automatic peak fitting, the

carbonyl peak was then moved slightly to obtain a good fit of the C 1s linescan. Subsequent carbon functional group peaks were then calculated from the total of the C 1s peak to give the carbon environment composition.

3. Results and Discussion

3.1 Scaffold morphologies using single surfactants: Span 80, PS-PEO, PS-PAA and PBD-PAA

Span 80 -The synthesis and characterization of styrene/divinylbenzene have been studied extensively in the literature[37, 38, 64] and as such, its discussion will be limited. The use of Span 80 surfactant here served as the control low molecular weight surfactant. There are several parameters that affect the scaffold. This is generally controlled at the emulsion stage as the structure of the parent emulsion is directly related to the final structure and morphology. Here, two important parameters are presented; effect of surfactant concentration and divinylbenzene crosslinking density. Increasing surfactant concentration from 10 wt/wt% to 50 wt/wt% of the oil phase has the macroscopic effect of decreasing the average void diameter. This is expected as the higher the surfactant concentration, the lower the interfacial tension. However, there is a critical concentration (80% reported)[65] where the voids are no longer interconnected and the foam is just a porous material. Another noticeable feature is that as the surfactant concentration increases, the interconnect size increases.

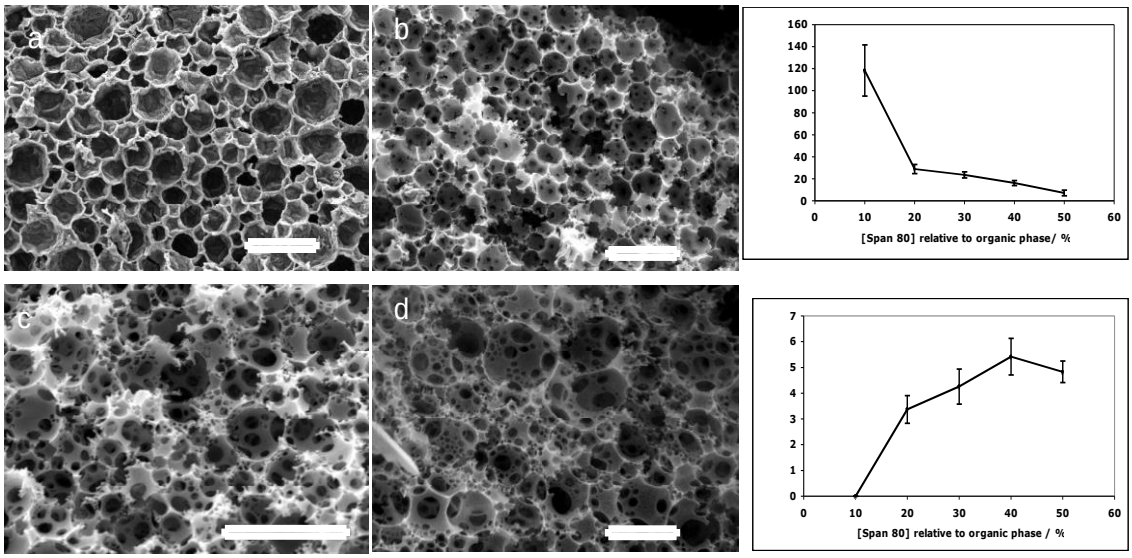

Figure 5. Right: Effect of surfactant concentration a) 10 wt/wt% low magnification b) 10 wt/wt% high magnification. c) 20 wt/wt% d) 30 wt/wt% e) 50 wt/wt%. Scale bars: a) 500 μm b→d) 50 μm e) 10 μm. Left: Graph representing macroscopic effect of surfactant concentration on average void and interconnect diameters. Error bars represent standard deviation.

It has been hypothesized that an increase in surfactant concentration is important in causing thinning of the organic thin film and the occurrence of interconnects appears

upon the curing of the emulsion[66] (approx 2.5 hours). This means the adjacent water droplets have to undergo rupture, which occurs during polymerization, a well documented vinyl chemistry phenomenon[38]. It is important to note that there is no bulk shrinkage of the polymer, the contraction is wholly internal (between adjacent droplets). Importantly, the ratio between void diameter and interconnect diameter is an indication of the overall porosity. Therefore, as the surfactant concentration increases the overall effect is an increase in porosity.

Emulsion parameters such as composition greatly affects its stability and morphology. An easy method to understand compositional effects of the external phase is varying the concentration of the crosslinker, DVB in this case. By increasing the concentration from 10-50 wt/wt% of the total organic, the main effect seen is the loss of interconnectivity of the foam while average void diameters remain roughly the same (~29–32 μm). The decrease in average interconnect diameters due to the presence of crosslinker, reduces the motility of the monomer and the surfactant within the oil phase effectively trapping the configuration of the foam at the early stages of polymerization[67]. However, it has been reported that an increase in DVB concentration from 0 to 80 wt/wt% resulted in a small increase in void diameters which is explained by the nature of the crosslinker. DVB is more hydrophobic than styrene making the emulsions more stable given that the immisciblity of the two phases is greater and the more stable the emulsion, the smaller the droplets.

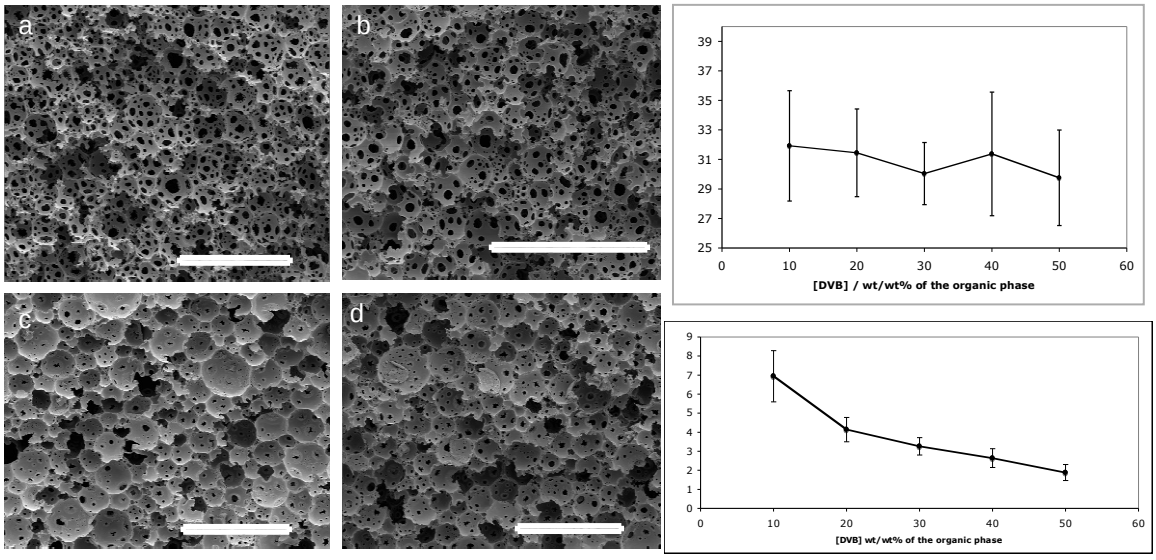

Figure 6. Left :Effect of divnylbenzene concentration. a→d 10, 20, 30 and 40 wt/wt% of the organic phase. Scale bars: 100 μm. Right: Graph showing macroscopic effect of divinylbenze on average void diameters and interconnect diameters. Error bars represent standard deviation.

The use of Span 80 surfactant has been proven successful to make polyHIPEs and consequently 3D scaffolds. However, polyHIPEs made in manner are have the right porous nature, they lack of surface control and often require post-processing modification. For this reason, block copolymer surfactants were used instead. The plethora of chemistries (and therefore functionalities), molecular weights and architecture, necessitates the need to choose the right block copolymer surfactants. Our aim is to design polyHIPEs with controlled surface chemistry to elucidate the effects of cellular adhesion on these substrates. As discussed in the introduction, cell adhesion is controlled by highly regulated sequences of binding and inert sites, exquisitely organized at the nano scale[68]. We will attempt to mimic this, using two different types of polymers: protein repellent and cell inert poly(ethylene glycol) (PEG) also known as poly(ethylene oxide) (PEO)[69] and poly(acrylic acid) (PAA)[17]. We will ensure anchorage to the polyHIPE by using the block copolymers of PEO and PAA with both PS and PBD. While the former will ensure anchorage to the polyHIPE DVB matrix, the unsaturated carbon backbone of PBD will participate in the free radical polymerization that leads to the formation of the polyHIPE.

PS-PEO, PBD-PAA and PS-PAA- Emulsions prepared with block copolymers required much lower concentrations to stabilize HIPE formation as high molecular weight nature enable higher surface area per molecule than lower weight surfactants.

Firstly, the use of styrene monomer and aqueous phase volume greatly affected the stability of the resulting emulsions. When styrene concentration was increased from (from 0 wt/wt% - 90 wt/wt% of the total organic phase), and aquoues phase volume is increased from 74% to 95% the degree of phase separation increased such that stable emulsions for a 24 hour period at room temperature consisted of 100% DVB with a maximum aqueous phase volume of 80%. Therefore, this formulation was observed for all emulsions prepared. The reason for such a small window for formulation remains to be studied. SEM and confocal laser scanning micrographs show the porous nature of the foams formed. There are several points to note however when comparing with Span 80 foams. Void diameters are much larger due to rapid coalescence of water droplets and show no apparent interconnectivity. Droplet coalescence (kinetic effect) and Ostwald ripening (thermodynamic effect) are the two main factors that contribute to emulsion destabilization. Coalescence of the water droplets is reported to be a consequence of the thinning and rupture of the thin film

(oil-phase) separating them[70]. While Ostwald ripening is the process by which large droplets grow at the expense of smaller ones because they are more energetically favourable. As a result, smaller droplets diffuse through the continuous phase and are re-deposited as larger droplets[71].

The macroscopic effect of Ostwald ripening is the gradual coarsening of the emulsion leading to an increased rate in droplet coalescence and eventual break down in the emulsion. Controlling these two processes during emulsion preparation ensures desired foam morphologies. In this case, although droplets coalesce to produce larger void diameters, there is little or no rupture of the oil-phase that leads to interconnect formation suggesting that Ostwald ripening is likely to be the dominant factor. To decrease the interfacial tension, the surfactant concentration may be increased. Unlike Span 80 however, increasing block copolymer concentration did not yield lower void diameters due to increased stability of the emulsions as before. In fact, an increase in PS-PEO concentration to 5 wt/wt% (DVB:PS-PEO = 3800:1) resulted in foams with highly convoluted and folded void morphology and above this concentration, macroscopic phase separation was observed. This is probably due to the molecular weight of the block copolymers. Increasing the number of the hydrophilic blocks , especially for charged blocks such as PAA, will increase the repulsions between the polymer chains, leading to phase separation. Regardless, The ability to form large voids in the order of 100 μm is advantageous for the cell culture applications.

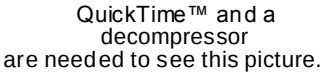

Figure 7. Divinylbenzene foams with the surfactants PS-PEO, PS-PAA and PBD-PAA. Top row: Confocal images showing porosity of the foams. No labelling was used as foams were auto fluorescent in green. d)-f) Low magnification SE images showing foam morphology and g)-i) high magnification of the interface showing DVB latex formation.

Although there is no macroscopic phase separation, SEM images revealed microscopic phase separation occurring at the interfaces by forming poly(DVB) latex particles for all block copolymer surfactants used (PS-PEO, PS-PAA, PBD-PAA). This is probably due to the inefficiency of block copolymers as surfactants to stabilize water-in-oil emulsions. When a 50 v/v% mixture of water/DVB with block copolymer (PS-PEO, PS-PAA of various concentration) solubilized in the oil phase, was manually agitated, oil-in-water emulsions spontaneously formed suggesting the preference for oil-in-water emulsion formation instead. This is in contrast to Span 80, which spontaneously forms water-in-oil emulsions. Therefore, during polymerization at high temperatures over a period of 24 hours allows sufficient time for the oil phase to diffuse across the interface, depositing DVB particles in the aqueous phase. Although, this is undesirable, it provides a platform for controlling the rate of diffusion of such DVB particles and thereby effectively controlling the topology at the oil/water interface.

3.2 Two surfactant HIPE system – PS-PEO and PS-PAA

3.21 Macroscopic and microscopic morphologies

The use of multiple surfactants to improve emulsion stability has been previously reported[41] Here, the use of mixed surfactant formulations is although aimed to control the topology of the surface via phase separation of the two block copolymers. Scanning electron micrographs reveal the porous nature of the scaffolds (Figure x). Furthermore, topographical features (particles) like those observed with PEO 100 foams for all compositions prepared (Figure x). However, No significant differences in topology was observed with a change in block copolymer chemistry (Appendix figure A-1)

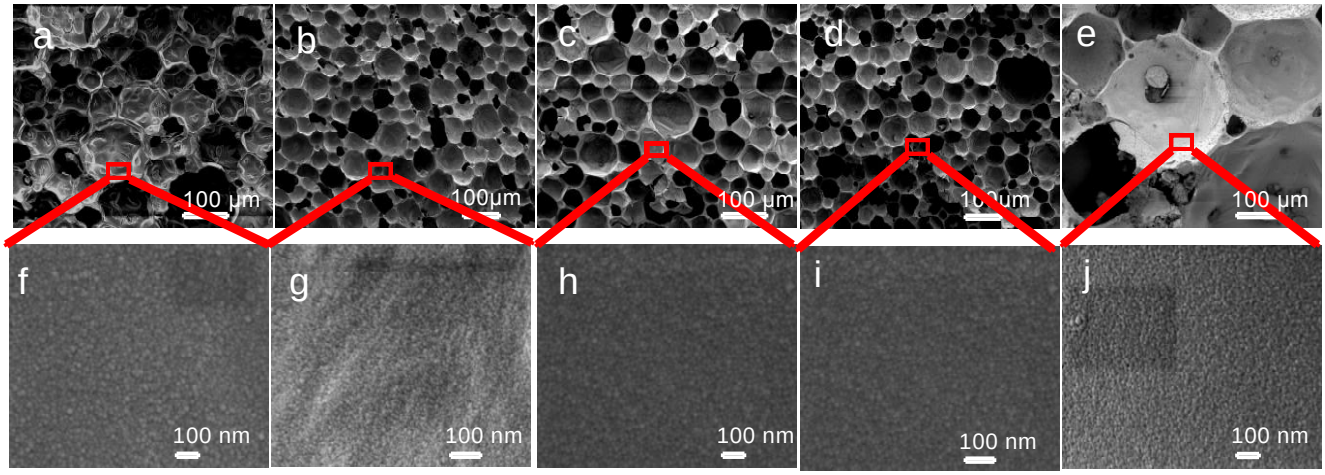

PEO 100 | PEO 75: PAA 25 | PEO 50:PAA 50 | PEO 25:PAA75 | PAA 100

Figure 8. Scanning electron micrographs of foam morphologies using mixed block copolymer compositions. Top row a)-e): low magnification. Bottom row f)-j): high magnification

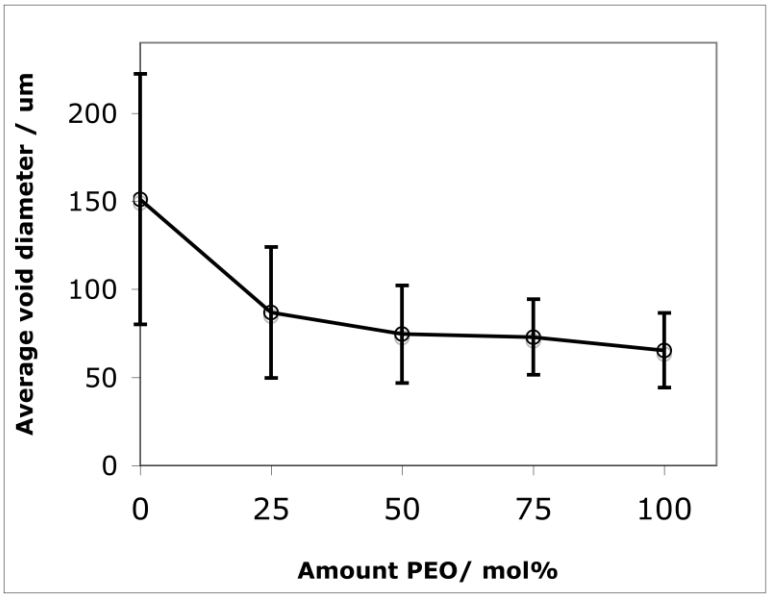

Figure 9. Average void diameters of DVB foams consisting of PS-PEO, PS-PAA and their mixtures, plotted as a function of PS-PEO content.

3.22 Porosity and Permeability of block copolymer scaffolds

Porosity and permeability are key components of a scaffold primarily for transport and removal waste metabolic products. To assess the level of 3 dimensional porosity, μCT was carried out on foams containing PEO100, PEO 50:PAA 50 and PAA 100. A representative 3D model is shown in Figure 9 and porosities calculated using the software package, are tabulated below.

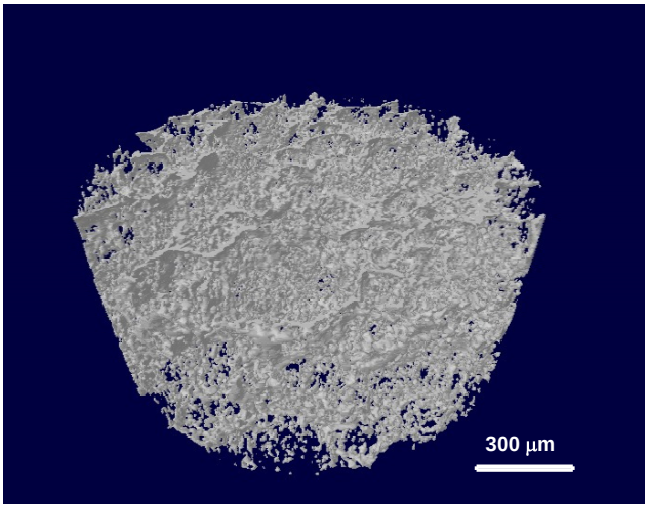

Figure 10. A representative 3D micro CT model of a divinylbenzene foam with PEO:50 PAA:50 surfactant composition. The model was created using the adaptive rendering algorithms.

	DVB matrix volume / %	Porosity / %	Pore strut thickness / μm	Pore diameter/ μm
PEO 100	9.49	90.5	10.7	32.9
PEO 50:PAA 50	7.46	72.5	9.80	38.9
PAA 100	3.30	96.7	9.70	194.5

Table 1. Open porosities of foams with block copolymer surfactants of PS-PEO, PS-PAA and a 50:50 mixture of the two surfactants. DVB matrix volume represents the total volume occupied by the DVB matrix in the selected region of interest.

Although % porosity maybe overestimated due to the resolution of the micro CT technique, 3D modelling enables us to visualize the level of porosity compared to SEM image analysis.

3.3 Characterization of Surface Chemistry and Wettability

The soxhlet extraction process although necessary for the removal of salts and unreacted monomers, is also responsible for the removal of surfactants and such is the case with conventional surfactants[62]. It was therefore necessary to characterize the surface chemistry to confirm the presence of the block copolymers (PS-PEO, PBD-PAA and PS-PAA) post purification.

XPS is a sensitive technique that allows for the characterization of the top 40 nm of a surface. The wide scan for each of the surfactants show peak positions for C and O only (with the exception of Span 80 that showed low levels Na and Si impurities). Since high-resolution spectra for the C 1s peaks were obtained, the presence of acid, ester or ether was analysed. Spectral assignments are listed below. The averaged C 1s peaks for PS-PEO (285.0 eV) and Span 80 (285.0 eV) is primarily due to C-C and C-H bonds the present in the PS/DVB matrix. The Span 80 molecule consists of a fatty acid ester that is clearly missing. The presence of oxygen in the wide scan most likely relates to the presence of water vapour within the sample. Similiarly, it is difficult to confirm the presence of the C-O ether group in PEO block as part of this signal may also be due to the presence of water vapour. However, measurements of contact

angles (see below) compliment the XPS data permitting us to validate part the C 1s signal coming from the ether.

The C 1s peaks are very different foams containing PBD-PAA and PS-PAA. The data shown here is for the purified foam. The C 1s peak is split with a major peak with a slight shoulder at 287eV and a smaller peak appearing at higher energy 289eV corresponding the C 1s in the C=O double bond. The major (averaged) peak consists of 3 separate signals. The biggest signal at 286 eV corresponds to C 1s in hydrocarbons (PS matrix), the smaller peak overlapping at 286 eV is from the C 1s of the C-OH single bond of the acid. Note that this peak intensity was made to correspond with the peak at 289 eV and is justified by the fact that the signal is coming the same C atom. Finally, the shoulder appearing at 287 eV corresponds to the C 1s from the α carbon (C-COOH). All peaks compare well with the literature[72, 73].

Finally, for foams consisting of PS-PAA surfactant, the XPS spectra albeit present the same peaks, the shoulder in the C 1s peak that represents the α carbon (C-COOH) and the smaller second peak that represents the C=O bond of the carboxylic acid are less defined probably owing to the fact PBD-PAA is a better surfactant whose chemistry is better retained on the surface of the foams.

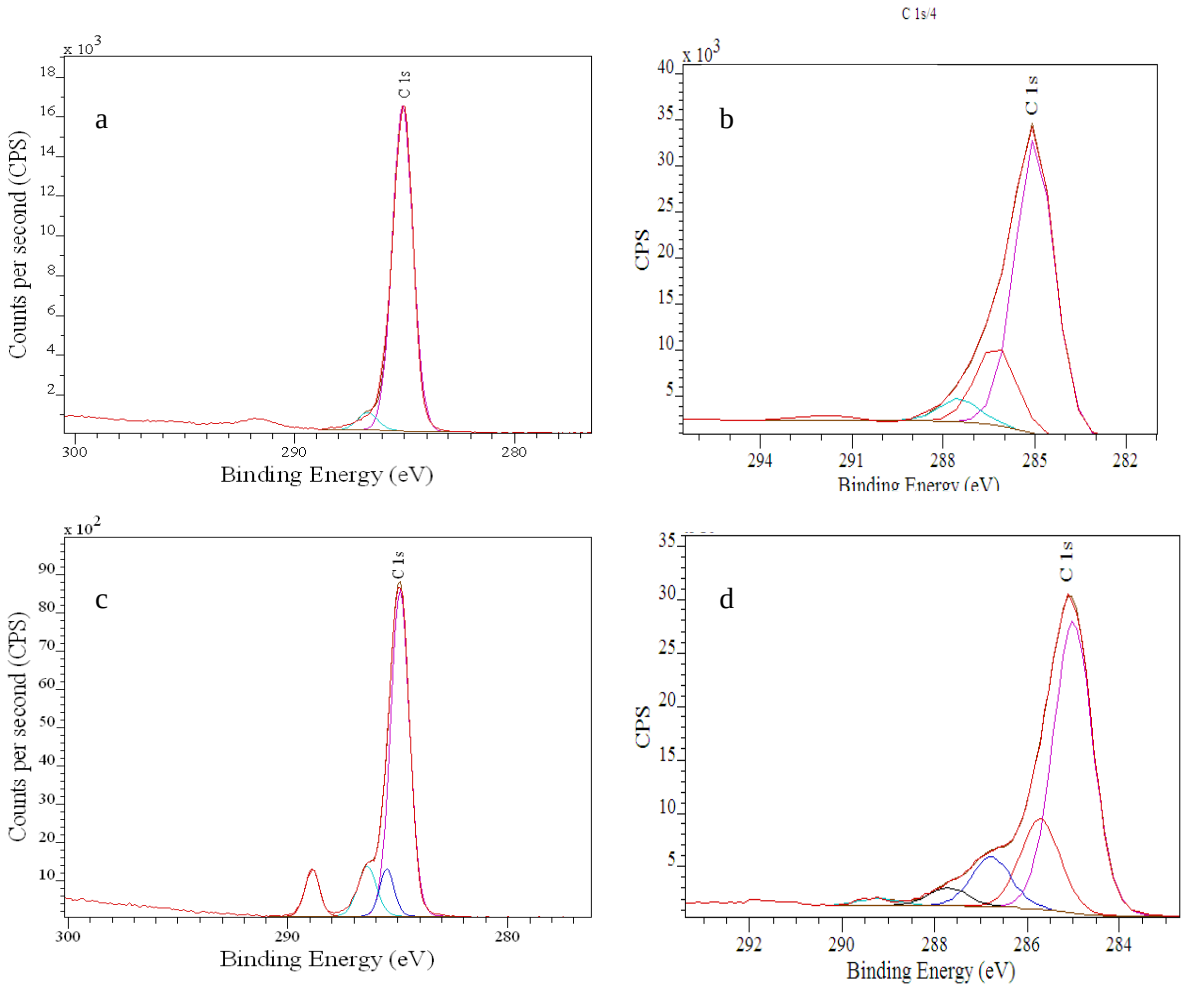

Figure 11. High resolution X-ray photoelectron spectra of C 1s peak of foams with a) Span 80, b)PS-PEO, c) PBD-PAA and d) PS-PAA.

	Binding Energy (eV) of C1s	Atomic %	Binding Energy (eV) of O1s	Atomic %
Span 80	285.0	86.64	529.0	6.848
PBD-PAA	285.0	85.64	529.0	14.35
PS-PEO	285.0	82.05	532.6	15.93
PS-PAA	285.0	88.49	532.6	9.430

Table 2. XPS spectral assignments and atomic weight % of Span and block copolymer surfactants.

From the XPS data presented, it is clear that the presence of acrylic acid groups is better defined with the PBD-PAA block copolymer. In this case, the hydrophobic block (1,4-butadiene) consists of an unsaturated C=C that is able to effectively co polymerize with the DVB matrix and therefore constrains the entire block copolymer at the interface and thereby preventing it from being washed out during purification.

With regards to PS-PEO and PS-PAA, the polymeric nature as well as the molecular weight of the surfactant also becomes important. In a polymer melt or in solution, polymer chain entanglements occur. These are essentially polymer chains interlocking as a result of chain overlap. The number of entanglements is directly proportional to the polymer chain length or molecular weight and in solution, its concentration and volume fraction. For PS-PAA, M_W for PS is 6.2 kDa and for PS-PEO, M_W for PS is 23 kDa. Since the PS block resides in the oil phase of the emulsions, it is confined in a thin film and in a small volume, allowing for such entanglements to occur, a phenomenon unavailable to short chain amphiphiles such as Span 80.

To confirm a true change in macroscopic surface wettability (particularly for PS-PEO functionalized foams) a series of contact angle measurements were made for foams of all surfactant compositions (Figure 11).

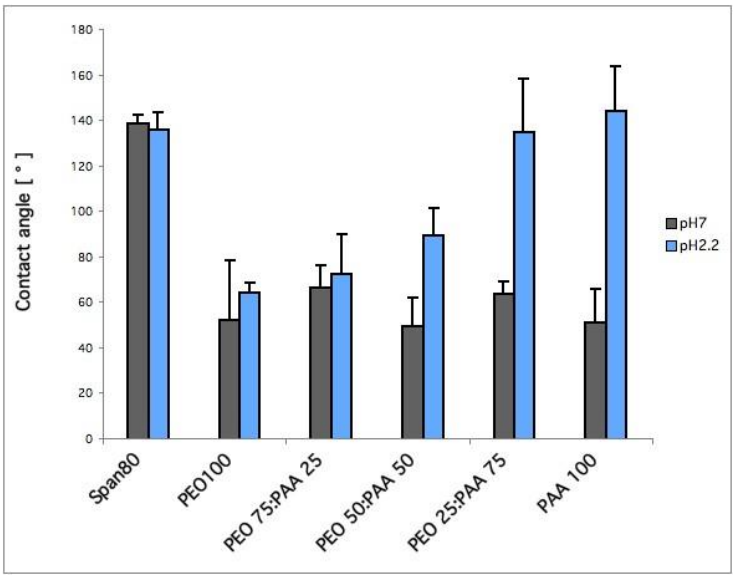

Figure 12. Contact angle measurements of foams comprising of Span 80, the block copolymers PS-PEO, PS-PEO and their mixtures at pH 7 and pH 2.2

These measurements give us important information; that there is macroscopic change in surface wettability. Foams with Span 80 are highly hydrophobic (138.25 ± 3.9).

Although foams with block copolymers are not highly hydrophilic (at pH 7), the massive change in hydrophilicity however verifies the presence of either PEO or PAA groups on the surface. Measurements at pH 2.2 were taken for two reasons; firstly, the pKa of the PAA block is ≈ 5.5. Above this pH, the acid groups are deprotonated and very hydrophilic. Below this pH, the acid groups remain protonated and are very hydrophobic. This is evidenced by the increase in contant angle as the molar ratio of PAA is increased. Secondly contact angles are not necessarily a measurement of surface tension when the surface of the substrate is not perfectly smooth. This is particularly relevant for the foams analyzed here. Those with Span 80 have different porosities and surface roughness than those with PS-PEO and PS-PAA affecting the true values of the measurements. But, this is compensated by taking measurements at two different pHs, making the results highly comparable.

3.4 Controlling surface topology through reaction kinetics

PS-PEO was chosen as the block copolymer surfactant while Span 80 was kept as the low molecular weight control. As the polymerization temperature was changed from room temperature then 40°C to 80°C several observations are notable. The porous nature of the foams (for both PS-PEO and Span 80 surfactants) remain unchanged. There were no significant differences in average void diameters within foams prepared with PS-PEO. Foams prepared with Span 80 from 40°C - 80°C however at room temperature, much larger (71 μm ± 26). Morphological differences in the foams were observed on the surface of the pores. The use of PS-PEO as a block copolymer surfactant is not entirely efficient for water-in-oil emulsions. For all foams prepared there is a degree of DVB diffusion across the interface, perhaps due to droplet coalescence, resulting in oil-in-water emulsion polymerization and the formation of latex particles (Figure x). The surface roughness and topology presented at the interface is explained by the nucleation of such latex particles but have not bud off the surface to form discrete latex particles. The diffusion of DVB and the formation of these particles (both size and polydispersity) are dependent on the temperature of polymerization and the rate of cross-linking, which are competing factors. The higher the temperature, the greater the diffusion and hence expected increase in number of particles. However, an increase in temperature also increases the rate of cross-linking, effectively trapping the formation of the particles at the interface. By systematically

varying the temperature of polymerization, we demonstrated that the size and dispersity of the topographical features could be controlled. Image analysis of the SE micrographs shows that as the temperature is increased, the size of the topographical features decreases and become more monodisperse.

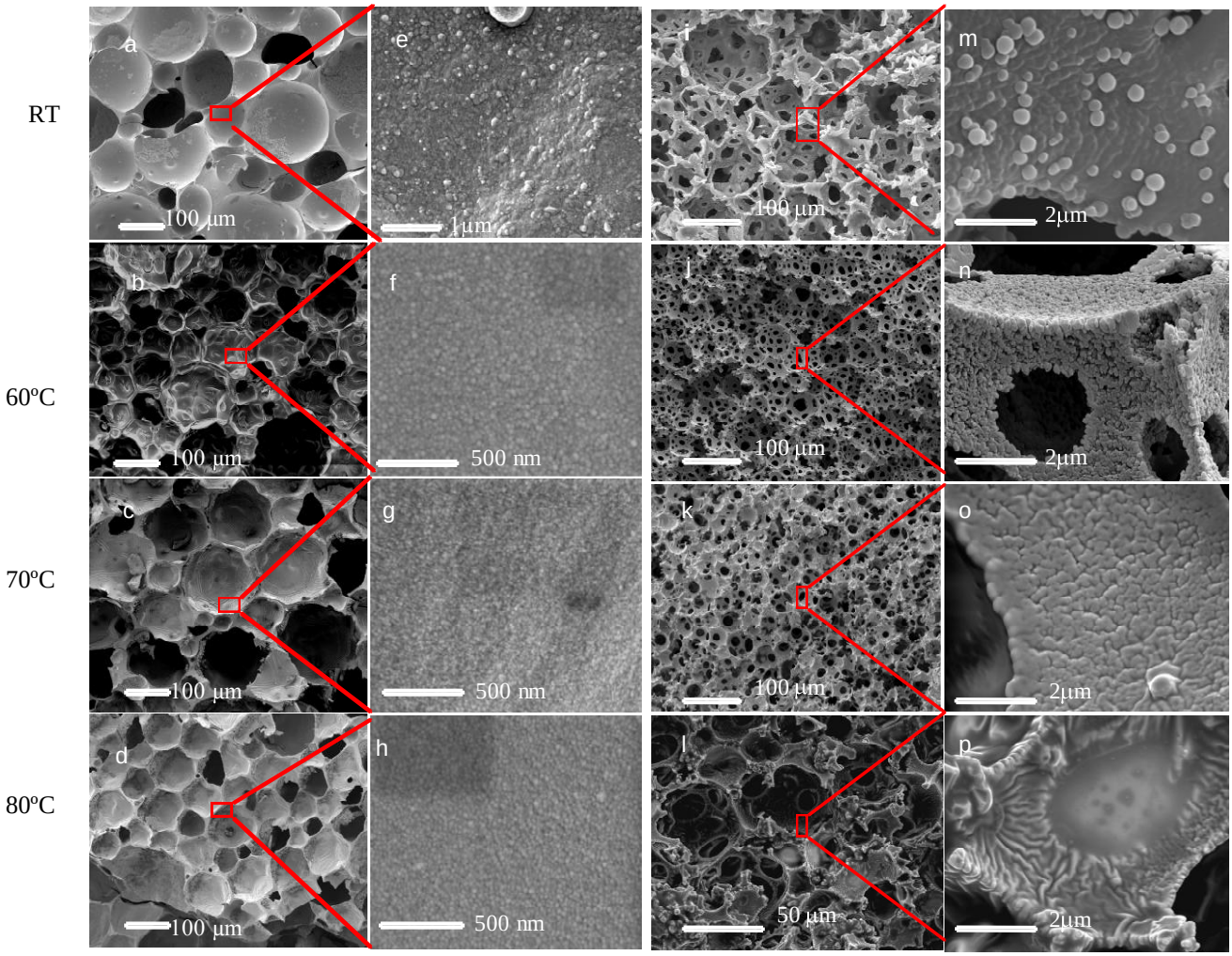

Figure 13. SE micrographs of foams containing PS-PEO (left) and Span 80 (right) surfactants at various temperatures. a)-d) low magnification of PS-PEO foams. e)-h) high magnification of the pore surface. i)-l) low magnification of Span 80 foams and m)-p) high magnification of the pore surface.

Foams with Span 80 however, only display such behaviour when polymerization is carried out room temperature and at 40 ºC. Beyond this temperature, the surface of the foams show a wrinkle effect. The oil-water interfaces in this case is more flexible leading to destabilization and allowing for a greater change in surface topology. The oil-water interfaces with block copolymer surfactants such as PS-PEO on the other hand seem to be more rigid, making changes on the pore surface subtler.

a

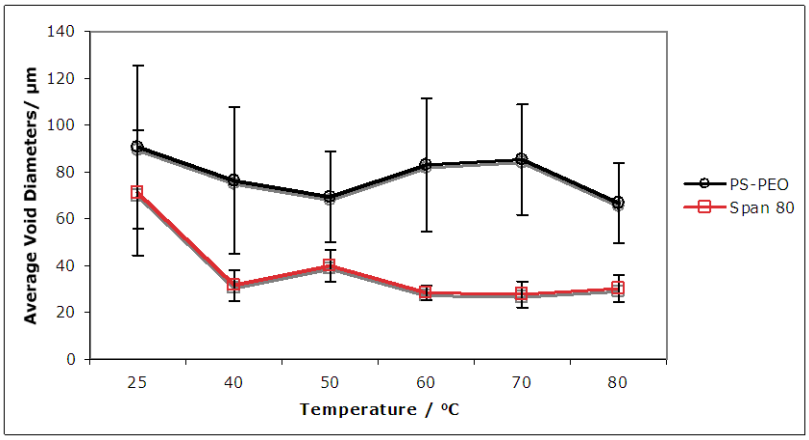

b

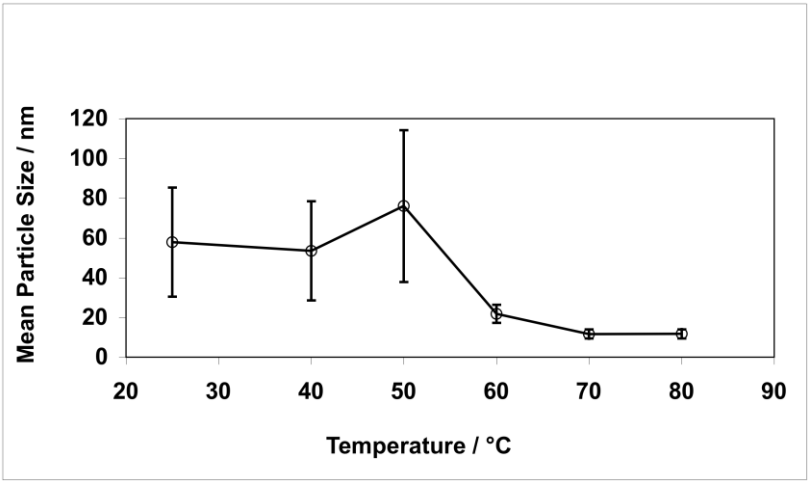

Figure 14. Top (a): Average void diameters of foams containing PS-PEO and Span 80 surfactants as a function of polymerization temperature. Void diameters were calculated from SEM image analysis. Bottom (b): Average particle size measured on the pore surface of PS-PEO foams as a function of polymerization temperature. Particle size and polydispersity decreases as temperature increases.

4. Conclusions

We have shown that emulsion templated scaffolds can be successfully prepared with block copolymers polystyrene-b-poly(ethylene oxide), polystyrene-b-poly(acrylic acid) and poly(1,4-butadiene)-b-poly(acrylic acid). While such emulsion templating provides an easy route to preparing scaffolds with tunable physical properties, their macroscopic architecture such as porosity and interconnectivity still need improvement. This is particularly important for biological characterization as long-term cell viability is required. Despite this, the scaffold surfaces were functionalized by the hydrophilic block of the copolymer surfactant in 3D, which cannot be obtained by using their small molecular weight counterparts such as Span 80. The use of multiple surfactants not only increases emulsion stability but also allows us to achieve functionalities (PS-PEO vs PS-PAA) and their properties (non-fouling vs adhesive) in discrete domains 3D environment. Additionally, the surface topography and polydispersity was also effectively controlled in 3D simply varying the polymerization temperatures.

Many of these scaffold features (surface chemistry, topology and stiffness) are important cues for cellular fate decisions. Therefore polyHIPE systems using block copolymer surfactants may provide the ideal 3D scaffold environment to understand the synergism of these cues towards hMSC differentiation for *in vitro* cell culture.

5. Appendix

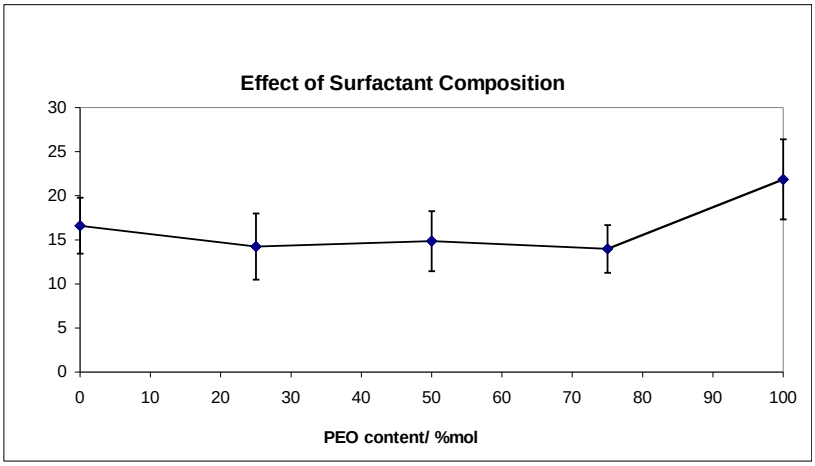

Figure A1. Graph representing surface topographical features of DVB foams with block copolymer mixture of PS-PEO and PS-PAA. No significant differences seen as a function of loss of PEO chemistry.

6. References

1. McBeath, R., Pirone, D.M., Nelson, C.M., Bhadriraju, K. & Chen, C. Cell Shape, Cytoskeletal Tension and RhoA Regulate Stem Cell Lineage Commitment. *Dev. Cell* **6**, 483-495 (2004).

2. Karlsson, C. *et al.* Human embryonic stem cell-derived mesenchymal progenitors-Potential in regenerative medicine. *Stem Cell Res.* (May 2009).

3. Pittenger, M.F. *et al.* Multilineage potential of adult human mesenchymal stem cells. *Science* **284**, 143-147 (1999).

4. Deng, J., Petersen, B.E., Steindier, D.A., Jorgensen, M.L. & Laywell, E.D. Mesenchymal stem cells spontaneously express neural proteins in culture and are neurogenic after transplantion. *Stem Cells* **24**, 1054-1064 (2006).

5. Patino, M.G., Neiders, M.E., Andreana, S., Noble, B. & Cohen, R.E. Collagen as an implantable material in medicine and dentistry. *J. Oral Implantol* **28**, 220-225 (2002).

6. Currie, L.J., Sharpe, J.R. & Martin, R. The use of fibrin glue in skin grafts and tissue-engineered skin replacements: A review. *Plast. Reconstr. Surg.* **108**, 1713-1726 (2001).

7. Handel, T.M. *et al.* Regulation of protein functions by glycosaminoglycans: As exemplified by chemokines. *Annu. Rev. Biochem.* **74**, 385-410 (2005).

8. Ruoslahti, E. & Pierschbacher, M.D. Arg-Gly-Asp: A Versatile Cell Recognition Signal. *Cell* **44**, 517-518 (1986).

9. Talhouk, R.S., Chin, J.R., Unemori, E.N., Werb, Z. & Bissell, M.J. Proteinases of the mammary gland: Developmental regulation in vivo and vectorial secretion in culture. *Development* **112**, 439-449 (1991).

10. Discher, D.E., Mooney, D.J. & Zandstra, P.W. Growth Factors, Matrices and Forces Combine and Control Stem Cells. *Science* **324**, 1673-1677 (2009).

11. Ingber, D.E. mechanical control of tissue morphogenesis during embrological development. *Int. J. Dev. Biol.* **50**, 255-266 (2006).

12. Peerani, R. *et al.* Niche-mediated control of human embryonic stem cell self-renewal and differentiation. *J. EMBO* **26**, 4744-4755 (2007).

13. Choi, N.W. *et al.* Microfluidic scffolds for tissue engineering. *Nat. Mater.* **6**, 908-915 (2007).

14. Martino, M.M. *et al.* Controlling inegrin specificity and stem cell differentiation in 2D and 3D environments through regulation of fibronectin domain stability. *Biomaterials* **30**, 1089-1097 (2009).

15. Arnold, M.A. *et al.* Activation of Integrin Function by Nanopatterned Adhesive Interface. *ChemPhysChem* **5**, 383-388 (2004).

16. Jiang, F., Horber, H., Howard, J. & Muller, D.J. Assembly of collagen into microribbons: effects of pH and electrolytes. *J. Struct. Biol.* **148**, 268-278 (2004).

17. Curran, J.M., Chen, R. & hunt, J.A. Controlling the phenotype and function of mesenchymal stem cells in vitro by adhesion to silane-modified clean glass surfaces. *Biomaterials* **26**, 7057-7067 (2005).

18. Freytes, D.O., Wan, L.Q. & Vunjak-Novakovic, G. Geometry and Force Control of Cell Function. *Journal of Cellular Biochemistry* **108**, 1047-1058 (2009).

19. Teixeira, A.I., Abrams, G.A., Bertics, P.J., Murphy, C.J. & Nealey, P.F. Epithelial contact guidance on well-defined micro- and nanostructered substrates. *J. Cell Sci.* **116**, 1881-1892 (2003).

20. Dalby, M.J. *et al.* The control of human mesenchymal cell differentiation using nanoscale symmetry and disorder. *Nat. Mater.* **6**, 997-1003 (2007).

21. Sordella, R., Jiang, W., Chen, G.C., Curto, M. & Settlemen, J. Modulation of Rho GTPase signalling regulates a switch between adipogenesis and myogenesis. *Cell* **113**, 147-158 (2003).

22. Engler, A.J., Sen, S., Sweeney, H.L. & Discher, D.E. Matrix Elasticity Directs Stem Cell Lineage Specificaion. *Cell* **126**, 677-689 (2006).

23. Stevens, M.M. & George, J.H. Exploring and Engineering the Cell Surface Interface. *Science* **310**, 1135-1138 (2005).

24. Shoichet, M.S. Polymer Scaffolds for Biomaterials Applications. *Macromolecules* **43**, 581-591 (2010).

25. Lutolf, M.P. & Hubbell, J.A. Synthetic biomaterials as instructive extracellular microenvironments for morphogenesis in tissue engineering. *Nat. Biotech.* **23**, 47-55 (2005).

26. Place, E.S. & George, J.H. Synthetic polymer scaffolds for tissue engineering. *Chem. Soc. Rev* **38**, 1139-1151 (2009).

27. Reilly, G.C. & Engler, A.J. Intrinsic extracellular matrix properties regulate stem cell differentiation. *Journal of Biomechanics* **43**, 55-62 (2010).

28. Oh, S.H., Park, I.K., Kim, J.M. & Lee, J.H. In vitro and in vivo characteristics of PCL scaffolds with pore size gradient fabricated by a centrifugation method. *Biomaterials* **28**, 1664-1671 (2007).

29. Pattison, M.A., Wurster, S., Webster, T.J. & Haberstroh, K.M. Three-dimensional, nano-structured PLGA scaffolds for bladder tissue replacement applications. *Biomaterials* **26**, 2491-2500 (2005).

30. Marklein, R.A. & Burdick, J.A. Spatially controlled hydrogel mechanics to modulate stem cell interactions. *Soft Matter* **6**, 136-143 (2009).

31. Wosnick, J.H. & Shoichet, M.S. Three-dimensional chemical patterning of transparent hydrogels. *Chem. Mater* **20**, 55-60 (2008).

32. Aizawa, Y., Leipzig, N., Zahir, T. & Shoichet, M.S. The effect of immobilized platelet derived growth factor AA on neural stem/progenitor cell differentiation on cell adhesive hydrogels. *Biomaterials* **29**, 4676-4683 (2008).

33. Li, W., Laurencin, C.T., Caterson, E.J., Tuan, R.S. & Ko, F.K. Electrospun nanofibrous structure: A novel scaffold for tissue engineering. *J. Biomed. Mater. Res.* **60**, 613-621 (2001).

34. Yoshimoto, H., Shin, Y.M., Terai, H. & Vacanti, J.P. A biodegradable nanofiber scaffold by electrospinning and its potential for bone tissue engineering. *Biomaterials* **24**, 2077-2082 (2003).

35. Xie, J. *et al.* The differentiation of embryonic stem cells seeded on electrospun nanofibers into neural lineages. *Biomaterials* **30**, 354-362 (2009).

36. Lissant, K.J. *J. Coll. Interf. Sci.* **22**, 462 (1966).

37. Zhang, H. & Cooper, A.I. Synthesis and applications of emulsions-templated porous polymers. *Soft Matter* **1**, 107-113 (2005).

38. Cameron, N.R. High internal phase emulsions as a route to prous polymers. *Polymer* **46**, 1439-1449 (2005).

39. Hayman, M.W., Smith, K.H., Cameron, N.R. & Przyborski, S.A. Enhanced neurite outgrowth by human neurons grown on solid three-dimensional scaffolds. *Biochem. Biophys. Res. Comm* **314**, 434-438 (2004).

40. Zhang, S. & Chen, J. Synthesis of open porous emulsion-templated monoliths using cetyltrimethylammonium bromide. *Polymer* **48**, 3021-3035 (2007).

41. Barbetta, A. & Cameron, N.R. Morphology and Surface Area of Emulsion Derived (PolyHIPE) Solid Foams Prepared with Oil-Phase Soluble Porogenic Solvent: Three Comoponent Surfactant System. *Macromolecules* **37**, 3202-3213 (2004).

42. Akay, G., Dawnes, S. & Price, V.J. Eur Pat Appl 1183328 A2. (2002).

43. Bokhari, M., Carnachan, R.J., Cameron, N.R. & Przyborski, S.A. Novel cell culture device enabling three-dimensional cell growth and improved cell function. *Biochem. Biophys. Res. Comm.* **354**, 1095-1110 (2007).

44. Cameron, N.R., Przyborski, S.A., Carnachan, R.J. & Bokhari, M. UK Pat Appl UK0608403.2. (2006).

45. Bokhari, M., Akay, G., Zhang, S. & Birch, M.A. The enhancement of osteoblast growth and differentiation in vitro on peptide hydrogel-polyHIPE polymer hybrid material. *Biomaterials* **26**, 5198-5208 (2005).

46. Akay, G., Birch, M.A. & Bokhari, M. Microcellular polyHIPE polymer supports osteoblast growth and differentiation bone formation. *Biomaterials* **25**, 3991-4000 (2004).

47. Bokhari, M., Carnachan, R.J., Przyborski, S.A. & Cameron, N.R. Emulsion-templated porous polymers as scaffolds for three dimensional cell culture: effect of synthesis parameters on scaffold formationa dn homogeneity. *J. Mater. Chem* **17**, 4088-4094 (2007).

48. Bokhari, M., Carnachan, R.J., Cameron, N.R. & Przyborski, S.A. Culture of HepG2 liver cells on three dimensional polystyrene scaffolds enhances cell structure and function during toxicological challenge. *J. Anat* **211**, 567-576 (2007).

49. Edwards, C.J.C., Gregory, D.P. & Sharples, M. Eur Pat Appl 239360. (1987).

50. Cameron, N.R. & Sherrington, D.C. Preparation and glass transition temperature of elastomeric PolyHIPE materials. *J. Mater. Chem.* **7**, 2209-2212 (1997).

51. Baker, S.C., Rohman, G., Southgate, J. & Cameron, N.R. The relationship between the mechanical properties and cell behaviour on PLGA and PCL scaffolds for bladder tissue engineering. *Biomaterials* **7**, 1321-1328 (2009).

52. Busby, W., Cameron, N. & Jahoda, A.B.C. Tissue Engineerin Matrices by Emulsion Templating. *Polym. Int.* **51**, 871-881 (2002).

53. Christanson, E.M., Soofi, W., Holm, J.L., Cameron, N.R. & Mikos, A.G. Biodegradable Fumerate based polyHIPEs as Tissue Engineering Scaffolds. *Biomacromol* **8**, 3806-3814 (2007).

54. Canal, C. *et al.* Topographical and Wettability Effects of Post Discharge Plasma Treatments on Macroporous Polystyrene-Divinylbenzene Solid Foams. *Plasma Processes and Polymers* **6**, 686-692 (2009).

55. Cummins, D. *et al.* Click chemistry as a means to functionalize macroporous PolyHIPE. *Soft Matter* **5**, 804-811 (2008).

56. Muller, A.H.E. & Matyjaszewski, K. *Controlled and Living Polymerizations: From Mechanisms to Applications*. (Wiley-VCH Verlag GmbH & Co., Weinheim; 2009).

57. Smart, T. *et al.* Block copolymer nanostructures. *Nano Today* **3**, 38-46 (2008).

58. Tadros, T. Polymeric surfactants in disperse systems. *Adv. Coll. Interf. Sci.* **147**, 281-289 (2009).

59. Reiss, G. & Labbe, C. Block copolymers in emulsion and dispersion polymerization. *Macromol. Rapid Commun.* **25**, 401-435 (2004).

60. Cameron, N.R. & Sherrington, D.C. Non aqueous high internal phase emulsions- preparation and stability. *J. Chem. Soc. Faraday Trans.* **92**, 1543-1547 (1996).

61. Mork, S.W., Rose, G.D. & Green, D.P. High-Performance Poly(butylene oxide)/poly(ethylene oxide) Block Copolymer Surfactants for the Preparation of Water-in-Oil High Internal Phase Emulsions. *J. Surfact. Deterg.* **4**, 127-134 (2001).

62. Lumelsky, Y., Lalush-Michael, I., Levenberg, S. & Silverstein, M.S. A degradable, porous, emulsion-templated polyacrylate. *J. Polym. Sci. A:Polym. Chem.* **47**, 7043-7053 (2009).

63. Massignani, M. *et al.* Controlling Cellular Uptake by Surface Chemistry, Size and Surface Topology at the Nanoscale. *Small* **5**, 2424-2432 (2009).

64. Ikem, V.O., Menner, A. & Bismarck, A. High internal phase emulsions stabilized solely by functionalized silica particles. *Angew. Chem. Int. Ed.* **47**, 8277-8279 (2008).

65. Williams, J.M. & Wrobleski, D.A. *Langmuir* **4**, 656 (1988).

66. Cameron, N.R., Sherrington, D.C., Albinston, L. & Gregory, D.P. Study of the formation of the open-cellular morphology of poly(styrene/divinylbenzne) polyHIPE materials by cryo-SEM. *Colloid Polym. Sci.* **274**, 592-595 (1996).

67. Lumelsky, Y. & Silverstein, M.S. Biodegradable Porous Polymers through Emulsion Templating. *Macromol* **42**, 1627-1633 (2009).

68. Geiger, B., Spatz, J.P. & Bershadsky, A.D. Environmental sensing through focal adhesions. *Nature Reviews Molecular Cell Biology* **10**, 21-33 (2009).

69. Blummel, J. Protein repellent properties of covalently attached PEG coatings on nanostructured SiO2- based interfaces. *Biomaterials* **28**, 4739-4747 (2001).

70. Friere, M.G. & Dias, A.M. *J. Interf. Sci.* **286**, 224-232 (2005).

71. Carnachan, R.J., Bokhari, M., Przyborski, S.A. & Cameron, N.R. Tailoring the morphology of emulsion-templated porous polymers. *Soft Matter* **2**, 608-616 (2006).

72. O'Toole, L., Beck, A. & Short, R.D. Characterization of Plasma Polymers of Acrylic Acid and Propanoic Acid. *Macromol.* **29**, 5172-5177 (1996).

73. Silva, R., Muniz, E.C. & Rubira, A.F. Multiple hydrophilic ultra-thin layers covalently anchored to polyethylene films. *Polymer* **49**, 4066-4075 (2008).